

# Launching and landing single molecular wheelbarrows on a Cu(100) surface

G. Rapenne<sup>a,\*</sup>, L. Grill<sup>b</sup>, T. Zambelli<sup>a</sup>, S.M. Stojkovic<sup>a</sup>, F. Ample<sup>a</sup>,  
F. Moresco<sup>b</sup>, C. Joachim<sup>a,\*</sup>

<sup>a</sup> NanoSciences Group, CEMES-CNRS, 29 rue Jeanne Marvig, P.O. Box 94347, 31055 Toulouse Cedex 4, France

<sup>b</sup> Institut für Experimentalphysik, Freie Universität Berlin, Arnimallee 14, 14195 Berlin, Germany

Received 26 July 2006; in final form 21 September 2006

Available online 28 September 2006

Dedicated to Prof. Guy Ourisson for his 80th birthday.

## Abstract

The sublimation of molecules under ultra-high vacuum conditions becomes critical with increasing molecular complexity as thermal fragmentation comes into play. In this case, scanning tunneling microscopy experiments of large molecules commonly focus on the small portion of the surface displaying intact molecules. In this work, we shed light on the major part of the surface where molecular fragments are observed. Upon the deposition of nanometer-sized wheelbarrows on a Cu(100) surface, only a few intact molecules, but several highly symmetric objects were observed. Using a full range of techniques the chemical structure and a possible formation pathway of these molecules were proposed.

© 2006 Elsevier B.V. All rights reserved.

The minimum size that a molecule should have to work as a machine is largely discussed in terms of both classical [1] and quantum [2] resources available. Applications for molecular electronics [3] and molecular mechanics [4] are discussed and the technology required to exchange energy and information with one and only the same molecule is also under debate [5]. However, when a molecule becomes large enough to embody for example a wheelbarrow [6,7], a nanocar [8] or a logic gate [9], it also becomes extremely difficult to bring it safe on the supporting surface by sublimation. From the crucible (the launching phase) to the surface (the landing phase), chemical reactions such as intramolecular reactions or fragment rearrangements can occur. By focussing the interpretation of the experiments on the few intact molecules on the surface, there is generally no mention of the chemical events which occur during the deposition.

In this Letter, the chemical events observed during the surface study of molecular wheelbarrows are detailed. Despite optimising the launching step to avoid many intramolecular reactions, we identify on the surface a trace contaminant coming from the original sample and new sequences of metal surface chemistry. To respect the atomic cleanness of the surface and the integrity of the molecule and since molecular complexity will increase in the future to achieve functional uni-molecular machines, we call for an extreme care in the deposition step.

Our experiments were performed on molecular wheelbarrows, a wheel-functionalised version of the Lander molecule series [10]. The design [6] and chemical synthesis [7] of this molecule have been described elsewhere. Presented in Fig. 1, the complexity of a C<sub>140</sub>H<sub>120</sub> wheelbarrow is reflected in its large molecular weight (1802 g·mol<sup>-1</sup>) which certainly makes its surface deposition challenging. Different deposition experiments were performed in an ultrahigh vacuum chamber with a base pressure of 10<sup>-10</sup> mbar. The Cu(100) substrates were cleaned by Ne ion sputtering and subsequent annealing at 770 K. For

\* Corresponding authors.

E-mail addresses: [rapenne@cemes.fr](mailto:rapenne@cemes.fr) (G. Rapenne), [joachim@cemes.fr](mailto:joachim@cemes.fr) (C. Joachim).

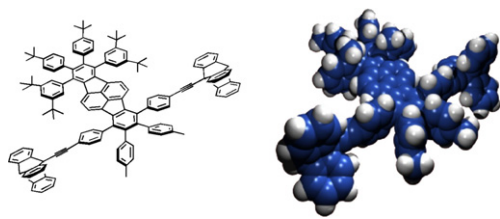


Fig. 1. The chemical structure and the 3D molecular model of the molecular wheelbarrow discussed.

the measurements with a homebuilt low temperature STM [11] the sample was cooled down to about 7 K. STM images were taken in constant-current mode and all bias voltages in this work are given with respect to the tip. A detailed understanding of the experimental results was obtained by comparison with calculated STM images. The Electron Scattering Quantum Chemistry (ESQC) method [12] associated with a molecular conformation optimisation on the surface was used to extract the effective stable conformation of a given STM-imaged molecule by making the calculated image converge scan by scan towards the experimental image.

In a first stage, the molecules were sublimed from a conventional Knudsen cell. It was necessary to heat the wheelbarrow powder up to 800 K to observe molecular structures on the Cu(100) surface. An example of an STM image recorded after this preparation is shown in Fig. 2. As one can see, only fragments of molecules can be imaged and no intact wheelbarrow molecule is visible on the surface. Therefore, the necessary sublimation temperature was high enough to cause fragmentation of the molecule. Among these fragments, a few ring-shaped objects were observed and their identity was later determined, as discussed below. In our design, the required two rotating wheels are linked to the central board of the

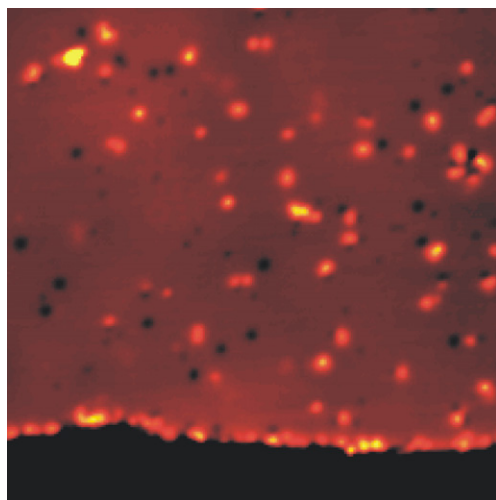


Fig. 2. A typical STM image of the Cu(100) surface after a Knudsen cell sublimation of molecular wheelbarrows (evaporation at 800 K). Many unidentified fragments and a few dimers are imaged (image size: 50 nm × 50 nm;  $I = 0.2$  nA,  $U = 0.7$  V).

wheelbarrow with thermally sensitive triple bonds. At high temperatures, these alkyne groups are reactive [13], causing a partial destruction of the molecular wheelbarrow during the deposition.

In a second stage, we have taken advantage of the known difference between the decomposition and sublimation rates of a large molecule [14]. A plot of these rates (in number of events per time unit) as a function of the temperature does not in general present the same slope, as presented in Fig. 3a. Although the base rate  $f_0$  and activation energy  $E_0$  are unknown for the molecular wheelbarrow, we assumed the existence of a distinctive temperature regime where the desorption rate is larger than the fragmentation rate. When this regime is established during a very short time, intact molecules are deposited onto the surface because, by working under kinetic control, the previously dominating fragmentation is suppressed [14]. The implementation of this ‘rapid heating’ technique consists in

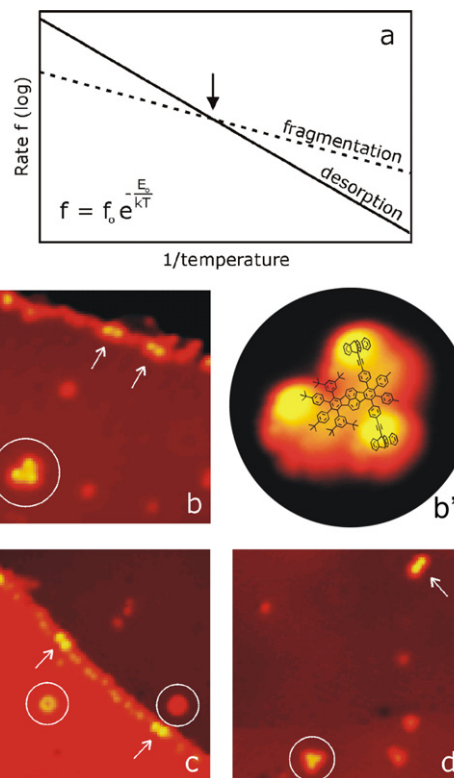


Fig. 3. The principle of the rapid heating procedure is presented in (a). The rates for fragmentation (dashed line) and desorption (solid line) are plotted as a function of  $1/\text{temperature}$ . The underlying equation is shown in the inset. The arrow indicates the temperature at which the desorption rate is equal to the fragmentation rate. (b), (c) and (d) are STM images (all  $20 \times 20$  nm<sup>2</sup> in size) of the corresponding Cu(100) surface after this rapid heating deposition of molecular wheelbarrows. In (b) the arrows indicate dimers adsorbed at a step edge ( $I = 0.2$  nA,  $U = 1$  V). An isolated wheelbarrow on a terrace is marked by a circle and shown separately (b') with its superimposed chemical structure (4 nm diameter,  $I = 0.2$  nA,  $U = 1$  V). (c) Dimers at the step edge and two tetramers, one on the upper terrace and one on the lower terrace ( $I = 0.2$  nA,  $U = 0.7$  V). (d) A trimer and a dimer (marked by a circle and an arrow, respectively) on the terrace ( $I = 0.2$  nA,  $U = 1$  V).

applying a short current pulse to a tungsten filament (0.25 mm in diameter) covered by molecules deposited beforehand by dipping the filament *ex situ* into a solution using a volatile solvent such as diethyl ether [15]. The filament was introduced into the ultrahigh vacuum chamber and positioned about 5 cm in front of the clean Cu(100) sample. Ideally, the pulse should be the shortest at the highest current. However, one must take into account the response time of the current generator and the maximum current tolerated by the filament before fusion. Satisfying results were obtained with current pulses of 600 ms duration at 6 A.

After depositing the molecules onto Cu(100) with this new procedure, we obtain the STM images presented in Fig. 3b–d. Intact molecular wheelbarrows are observed on flat Cu(100) terraces [16] and rod-like dimers are present mainly at the Cu(100) step edges (Fig. 3b). Moreover, isolated ring-shaped tetramers (Fig. 3c) and propeller-like trimers (Fig. 3d) can be distinguished. By lateral manipulation with the STM tip it is possible to move laterally and one at a time such objects on the Cu(100) surface. After the manipulation, done at tunnelling resistances between 100 and 400 k $\Omega$ , the intact structures were found at the desired position, confirming that each of them is a complete molecular object.

In Fig. 4 high resolution STM images of the three different highly symmetric objects present on the surface besides the wheelbarrows are shown and compared with calculated images. To explain the presence of the three different types

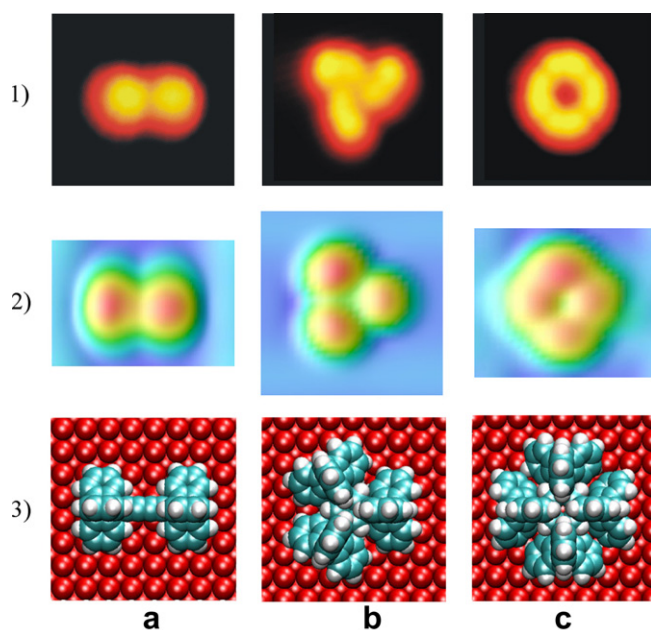


Fig. 4. Line 1: experimental STM images (all  $3 \times 3 \text{ nm}^2$  in size) of highly symmetric objects observed searching for molecular wheelbarrows: (a) the dimer, (b) the trimer and (c) the tetramer. Line 2: the corresponding ESQC constant current STM images after optimizing the adsorbed conformation of each molecule (all 3 nm-wide). Line 3: the corresponding optimized conformation corresponding to the best fit between the experimental and calculated STM images (all  $2 \times 2 \text{ nm}^2$  in size).

of structures some general considerations have to be done. First of all, concerning the dimer structures, one has to refer to the analytical tools used during the synthesis of the molecules. The wheelbarrow molecules were purified by preparative column chromatography and the product purity was determined to be higher than 99.5% by Nuclear Magnetic Resonance and High Pressure Liquid Chromatography. However, by mass spectrometry it was possible to detect a side-product of the wheelbarrow synthesis as trace contaminant, composed of two triptycene wheels connected by a  $\text{C}\equiv\text{C}-\text{C}\equiv\text{C}$  linker ('Dimer' in Fig. 5). To clarify if these trace contaminants appear in the STM images as the observed dimers, genuine triptycene dimer molecules were synthesized separately from pure ethynyl triptycene and investigated by STM under the same conditions. The observed molecules are identical in height and width with the previously observed dimers and thus confirm the interpretation. To further support this result, ESQC STM image calculations were performed to determine the conformation of triptycene dimer molecules on the Cu(100) surface, which unambiguously assign the objects found on the surface to triptycene dimers. A modified version of the ASED semi-empirical Molecular Orbital method was used to optimise the molecular conformation and the chemisorption distance to the surface [17]. The central molecular axle was found to be curved due to its interaction with the surface and the two triptycene wheels are flattened by their direct chemisorption on the Cu(100) surface.

To explain the relatively high number of wheel dimers on the surface (compared to wheelbarrows), it is noteworthy that the molecular mass of the dimer ( $555 \text{ g} \cdot \text{mol}^{-1}$ ) is much lower than the wheelbarrow one ( $1802 \text{ g} \cdot \text{mol}^{-1}$ ). Therefore, the lighter dimer molecules, which are present in the wheelbarrow solution deposited on the filament before the launching phase, are sublimed more easily and land in higher proportion on the surface. This is an example where a trace contaminant at the launching phase can be the major product observed upon landing.

Trimers (Fig. 4b) and tetramers (Fig. 4c) appear in the STM images as three and four bumps, respectively, which we assign to triptycene wheels. Fig. 5 shows the proposed chemical structures for the wheel trimer and the wheel tetramer. The corresponding STM images and the respective surface conformations have been calculated by ESQC following the same procedure as for the dimer. A very good agreement was obtained between the experimental and calculated images, confirming our chemical structure determination.

After sublimation of the separately synthesized wheel dimers on the Cu(100) surface, no tetramers and only few trimers were observed in the STM images. Therefore, we argue that the formation of the wheel trimer is amplified by the wheelbarrow and that the production of the wheel tetramer requires its presence. As observed previously [16], the wheelbarrow can be fragmented especially at the anchoring points of the wheels on the central board,

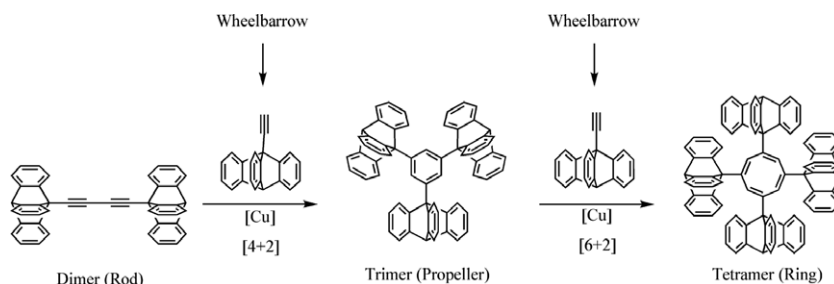


Fig. 5. Synthetic pathway to explain the formation of the trimer and tetramer molecules using as reactants both the wheel dimer and wheel fragments originating from the wheelbarrow.

because the design required rather reactive alkyne groups which, under the experimental conditions, yield reactive ethynyltritycene fragments (free wheels). Metal-catalysed cyclotrimerisation of alkynes to benzene derivatives has been extensively described [13]. Cobalt is the most common catalyst for such reactions [13], but copper can also be used [18,19]. A thermal  $[2 + 2 + 2]$  cyclotrimerisation of ethynyltritycene can be envisaged, as well as the  $[4 + 2]$  Diels–Alder cycloaddition between a dimer and the free wheel. Both routes could explain the formation of the wheel trimer but the first mechanism is entropically disfavoured since it would involve the reaction of three different partners. Therefore, the formation of the propeller-shaped trimer is considered to proceed through the  $[4 + 2]$  reaction of an ethynyltritycene fragment (free wheel) with the wheel dimer (first step of Fig. 5).

The formation of the wheel tetramer requires that the metal surface plays a unique role, not only by promoting this reaction but also by stabilising its antiaromatic eight-membered ring [20,21]. Four types of metal-catalysed cycloadditions lead to such rings, namely the  $[2 + 2 + 2 + 2]$ ,  $[4 + 2 + 2]$ ,  $[4 + 4]$ , and  $[6 + 2]$  reactions. Cycloaddition reactions involving three or more components are entropically highly disfavoured and therefore the  $[2 + 2 + 2 + 2]$  and  $[4 + 2 + 2]$  routes are unlikely. We rule out the  $[4 + 4]$  mechanism since no rings had been observed in the experiments performed on the pure wheel dimer. We therefore attribute the formation of the ring-shaped tetramer to a  $[6 + 2]$  addition of an ethynyltritycene fragment (free wheel) and the benzene ring of a previously formed propeller-shaped trimer (second step of Fig. 5).

In conclusion, a complex uni-molecular machine such as a molecular wheelbarrow was deposited intact onto a surface with the help of a specific sublimation procedure milder than the standard one using a Knudsen cell. During the launching phase however, low molecular weight contaminants constituted the major part of the launched molecules. While thermally activated fragmentation is minimized during the launching phase, the metallic surface acts as a catalyst for cycloaddition reactions, leading to the formation of highly symmetric molecules. The chemical structure of the cycloaddition products formed *in situ* has been elucidated with the help of molecular conformation

extraction using STM image calculations and a mechanism for the formation of the trimer and the tetramer has been proposed. This demonstrates that the deposition of a large molecule on a metal surface requires an extreme care in the launching and landing phases in order to minimize the intrusion of new molecules and trace contaminants. This phenomenon is likely to be severe for more advanced nanomachines which will integrate a larger variety of functional subunits.

#### Acknowledgements

We are grateful to the European Union (AMMIST RTN Program), CNRS and Université Paul Sabatier for financial support.

#### References

- [1] R. Baum, Chem. Eng. News 81 (2003) 37.
- [2] C. Joachim, Nanotechnology 13 (2002) R1.
- [3] C. Joachim, J.K. Gimzewski, A. Aviram, Nature 408 (2000) 541.
- [4] F. Moresco, G. Meyer, K.H. Rieder, H. Tang, A. Gourdon, C. Joachim, Phys. Rev. Lett. 87 (2001) 088302.
- [5] J.K. Gimzewski, C. Joachim, Science 283 (1999) 1683.
- [6] C. Joachim, H. Tang, F. Moresco, G. Rapenne, G. Meyer, Nanotechnology 13 (2002) 330.
- [7] G. Jimenez-Bueno, G. Rapenne, Tetrahedron Lett. 44 (2003) 6261.
- [8] Y. Shirai, A.J. Osgood, Y. Zhao, K.F. Kelly, J.M. Tour, Nanoletters 5 (2005) 2330.
- [9] I. Duchemin, C. Joachim, Chem. Phys. Lett. 406 (2005) 167.
- [10] F. Moresco, A. Gourdon, Proc. Nat. Acad. Sci. USA 102 (2005) 8809.
- [11] G. Meyer, Rev. Sci. Instrum. 67 (1996) 2960.
- [12] P. Sautet, C. Joachim, Chem. Phys. Lett. 185 (1991) 23.
- [13] S. Saito, Y. Yamamoto, Chem. Rev. 100 (2000) 2901.
- [14] R.J. Beuhler, E. Flanigan, L.J. Greene, L. Friedman, J. Am. Chem. Soc. 96 (1974) 3990.
- [15] T. Zambelli, P. Jiang, J. Lagoute, S. Gauthier, A. Gourdon, C. Joachim, Phys. Rev. B 66 (2002) 075410.
- [16] L. Grill, K.H. Rieder, F. Moresco, G. Jimenez-Bueno, C. Wang, G. Rapenne, C. Joachim, Surf. Sci. 584 (2005) 153.
- [17] F. Ample, C. Joachim, Surf. Sci. 600 (2006) 3243.
- [18] G. Borsato, O. De Lucchi, F. Fabris, L. Groppo, V. Lucchini, A. Zamboni, J. Org. Chem. 67 (2002) 7894.
- [19] J. Li, H. Jiang, M. Chen, J. Org. Chem. 66 (2001) 3627.
- [20] P.W. Jolly, in: G. Wilkinson, F.G.A. Stone, E.W. Abel (Eds.), Comprehensive Organometallic Chemistry, vol. 8, Pergamon, London, 1982, p. 649.
- [21] R.E. Colborn, K.P.C. Vollhardt, J. Am. Chem. Soc. 108 (1986) 5470.